The 19th Conference of Mechanical Engineering Network of Thailand
19-21 October 2005, Phuket, Thailand

Capability Assessment of Intermittency Transport Equations for Modeling Flow Transition

Keerati Suluksna [1], Varangrat Juntasaro [2] and Ekachai Juntasaro [1*]
[1] School of Mechanical Engineering, Institute of Engineering, Suranaree University of Technology, Nakhon Ratchasima 30000, Thailand
[2] Department of Mechanical Engineering, Faculty of Engineering, Kasetsart University, Bangkhen, Bangkok 10900, Thailand
*Email: junta@sut.ac.th

Abstract

The present paper is aimed to test and assess the capability of intermittency transport equations which are used to model the flow transition. Two popular models of the intermittency transport equations developed by two research groups are considered. The first model proposed by Suzen and Huang [1] is obtained from combining the best features of the Cho and Chung [2] model and the Steelant and Dick [3] model, and the second one proposed by Menter et al [4] is revealed in the form of a generalized intermittency transport equation. The frameworks of both models play an important role in modern CFD codes and are incorporated into the transition computation features of some well-known CFD commercial softwares such as CFX-v-1.0. In this paper, both transport equations are integrated into the SST k-ω turbulence model of Menter [5] and employed to predict the flat plate boundary layer flow with zero pressure gradient and different freestream turbulence intensities: T3AM, T3A and T3B. Detailed comparisons of the computational results with the experimental data of Coupland (1993) and with the computational results of the low-Reynolds number k-ε of Launder and Sharma [6] and the SST k-ω model of Menter [5] are presented.

Keywords: Intermittency, Transition, Boundary layer, Freestream turbulence intensity.

and comparing with the results of conventional turbulence models, the low-Reynolds number k-ε of Launder and Sharma (1974) and the SST k-ω model of Menter [12]

Nomenclature

f	generalized intermittency factor
FSTI	free stream turbulence intensity (%), u'/U_{in}
H	shape factor, δ^*/θ
k	turbulence kinetic energy
K_t	flow acceleration parameter, $(\nu/U^2)(dU/ds)$
Re_θ	momentum thickness Reynolds number, $\rho\theta U_\infty/\mu$
$Re_{\theta t}$	transition onset momentum thickness Reynolds number, $\rho\theta_t U_\infty/\mu$
$Re_{\theta c}$	critical momentum thickness Reynolds number
n	spot generation rate
s	streamwise coordinate
S	strain rate magnitude, $(2S_{ij}S_{ij})^{0.5}$
S_{ij}	voricity tensor, $0.5(\partial u_i/\partial x_j+\partial u_j/\partial x_i)$
Tu	turbulence intensity (%), u'/U
U	local velocity magnitude
y_n	distance normal to the nearest wall
γ	intermittency factor
δ^*	displacement thickness
θ	momentum thickness
μ	molecular viscosity
μ_t	turbulent eddy viscosity
ρ	density
σ	spot propagation parameter
ω	specific turbulence dissipation rate
Ω	vorticity magnitude, $(2\Omega_{ij}\Omega_{ij})^{0.5}$
Ω_{ij}	voricity tensor, $0.5(\partial u_i/\partial x_j-\partial u_j/\partial x_i)$

subscripts

in	inlet referent
t	onset of transition
∞	local freestream

1. Introduction

Flow transition plays an important role in the design and performance of turbomachinery applications and aerospace devices where the wall-shear-stress or wall-heat-transfer or both is of interest. Majority of boundary layer flows in turbomachines and airfoils involve flow transition under the effects of many factors, such as freestream turbulence, pressure gradient and separation, Reynolds number, Mach number, turbulent length scale, wall roughness, streamline curvature, heat transfer, etc. Prediction of this flow type is an important element in analysis and performance evaluation and ultimately in the design of more efficient turbomachines and aerospace vehicles [7]. Especially, for example, in low pressure turbine applications, the flow in the cascade passages can result in the boundary layer of the blade being laminar or transitional over 50-70% of the blade surface. In such circumstances, the transition process can have major operational consequences. It has been known that early transition may prevent separation (stall) of the suction-side boundary layer and consequently lead to a significant reduction in total-pressure loss [8]. As a result, the number of blades and stages may be reduced within turbomachinery to save cost. Furthermore, in case of aerospace devices, the transition process can also have a strong influence on the separation behavior of boundary layers leading to a large effect on the performance of airfoils and bluff bodies. For example, at low Reynolds number with low freestream turbulence, the boundary layers on the airfoil surface have a tendency to remain laminar and hence the flow may separate before it become turbulent. This may cause a drop in efficiency and result in an increase of fuel consumption. For all these reasons, the performance, weight and costs associated with turbomachines and many aerospace devices can be affected by transition and the prediction of its behavior is even more important for reasons of design efficiency [9].

At present, there are mainly three concepts used to model transition in industry. The first approach is based on the stability theory. The successful technique is the so-called e^N method. It is based on the local linear stability theory and the parallel flow assumption in order to calculate the growth of the disturbance amplitude from the boundary layer neutral point to the transition location. This method is not compatible with current CFD methods because typical industrial Navier-Stokes solutions are not accurate enough to evaluate the stability equation. In addition, since it is based on linear stability theory, it cannot predict transition due to non-linear effects such as high freestream turbulence or surface roughness. Therefore, this method is currently used for the case of natural transitions [7][9].

The second approach is the use of conventional turbulence model. One way is to switch on the turbulence model or eddy viscosity at an experimentally predetermined transition location. This method is *ad hoc* and ignores the transition physics and the importance of the transition zone completely. Especially for flows where the transitional region covers a large portion of the flow field, as observed in many low-pressure turbine experiments, this practice can lead to severe errors in the solution. Another way is to use of the low-Reynolds number turbulence models. However, for the last ten years, the ability of the turbulence models in predicting the transitional flows have been investigated by many research groups, such as ERCOFTAC SIG (1991-1993), Westin and Henkes (1997), etc., by testing a large variety of turbulence models and comparing model performance in predicting the transition flow experiments. The conclusions indicated that most of two-equation turbulence models even the Launder and Sharma model, which was found as the best performer in the category of two-equation turbulence models, gave unsatisfactorily too early transition onset point and too short transition length. In addition, the prediction performance was found to depend on the inlet conditions at the leading edge. This outcome is not a surprise since most of the current turbulence models are not designed to predict flow transition, and, in order to correctly predict the flows affected by transition, some special treatments were needed in turbulence models [7][10].

The third approach to predict transition, which is favored by the gas turbine industry, is to use the concept of intermittency to blend the flow from laminar to turbulent regions. The intermittency is the fraction of time the flow is turbulent during the transition phase, which is zero in the pre-transition region and becomes unity in the fully turbulence region, so that the start and development of transition can be imposed. The development of intermittency is quite general for steady flow on a flat plate and therefore the onset location and growth rate of transition can be correlated. Most correlations usually relate the freestream turbulence intensity, *Tu*, and the pressure gradient to the transition momentum thickness Reynolds number. A typical example is the correlation of Mayle [11], which is based on a large number of experimental observations. Another popular correlation is the Abu-Ghannam and Shaw [12] model, which additionally accounts for the influence of the pressure gradient.

In the early applications of the intermittency concept, the development of intermittency was described algebraically by the law of Dhawan and Narasimha [13] with the start and end of transition determined by correlations. However, this law is not appropriate for general applications, which are mostly under the effects of non-zero pressure gradients and high freestream levels, because it is valid only for the flow with zero pressure gradient and natural transition (freestream turbulence level < 1%). A more general intermittency is obtained by an intermittency transport equation. For example, the intermittency transport model of Steelant and Dick [3] is derived from the intermittency distribution of Dhawan and Narasimha [13] along the streamline direction. Another example based on the concept of local variables is formulated by Menter et al [4] in a form of a generalized intermittency variable. The concept of intermittency can be successfully incorporated into the turbulence model computation in many ways, such as in the framework of Steelant and Dick [3] the intermittency is incorporated into the two sets of the strongly coupled equations of conditionally averaged Navier-Stokes equations. This approach is too complex and not compatible with current CFD codes in which only one set of Navier-Stokes equations is involved. As a result, transitional flows are almost invariably modeled within a Reynolds Averaged Navier-Stokes (RANS) framework, and usually linked with the turbulence model by a modification of some terms in the turbulence model. Example of using the later approach is the use of intermittency obtained from the Dhawan and Narasimha correlation incorporated into the turbulence model introduced by Baek et al [10]. Another example is to use the transport equation for intermittency incorporated into the turbulence model introduced by Suzen and Huang [1], Menter et al [4], Pecnik et al [14], Lodefier et al [15], etc.

In the present study, the two different intermittency transport equations for modeling the transition are implemented. The first one was proposed by Suzen and Huang [1] (Suzen-Huang model) and the second one was developed by Menter et al [4] (Menter et al model). Both models are employed to predict the flat plate boundary layer with shape leading edge under zero pressure gradient and various freestream turbulence intensities.

The performance of both models is assessed by validating against the skin friction coefficient and shape factor of the Coupland (1993) experimental data and also comparing with the results of conventional turbulence models, the low-Reynolds number k-ε model of Launder and Sharma [6] (Launder-Sharma model) and the SST k-ω turbulence model of Menter [5] (Menter-SST model), to test their ability to simulate transition. Finally, the intermittency profiles of both models are observed and where in the boundary layer the intermittency of each model is activated on.

2. Transport Models for the Intermittency

In this study, two transition models with the transport equations of the intermittency factor are investigated, the first one is Suzen-Huang model and the second one is Menter et al model. Both models are integrated in conjunction with the Menter-SST model. Detailed information of both models are described as follows:

2.1 Transport model of Suzen and Huang

According to Suzen and Huang [1], the transport equation for the intermittency factor was developed based on the idea of combining the best features of the two existing transition models, the model of Cho and Chung [2] (Cho-Chung model) and the model of Steelant and Dick [3] (Steelant-Dick model). For near wall flows the Steelant-Dick model was chosen, which reproduces the streamwise variation of the intermittency factor in the transitional zone by using the relation of Dhawan and Narasimha [13]. For a realistic cross-stream variation of the intermittency factor the Cho-Chung model was taken, which was derived for free-shear flows. However, the Suzen-Huang model has been slightly adapted in some points afterward, and the new one in Suzen and Huang [16], is used here.

A general intermittency equation can be written as

$$\frac{\partial \rho u_j \gamma}{\partial x_j} = D_\gamma + S_\gamma \qquad (1)$$

with the diffusion term D_γ and the source term S_γ

$$D_\gamma = \frac{\partial}{\partial x_j}\left[(1-\gamma)(\gamma\sigma_{\gamma l}\mu + \sigma_{\gamma t}\mu_t)\frac{\partial \gamma}{\partial x_j}\right] \qquad (2)$$

$$S_\gamma = (1-\gamma)\left[(1-F)T_0 + F\left(T_1 - T_2\right)\right] + T_3 \qquad (3)$$

The blending function F is used to facilitate as a gradual switch from the Steelant-Dick model to the Cho-Chung model inside the transition region and is given as

$$F = \tanh\left[\frac{k/\Omega\nu}{200(1-\gamma^{0.1})^{0.3}}\right] \qquad (4)$$

It should be noted that in some applications the vorticity magnitude, Ω, in the blending function F can be replaced by the strain rate magnitude, S. However, Suzen (private communication) pointed out that both could be employed, but the use of the strain rate magnitude may cause a non-physical build-up of intermittency factor (and turbulence kinetic energy, k) in stagnation regions which is a well known problem of two equation turbulence models.

The production term T_0 comes from the Steelant-Dick model, aimed to reproduce the intermittency distribution of Dhawan and Narasimha. Two production terms T_1 and T_2 come from the Cho-Chung model, the term T_1 mimics the production of turbulence kinetic energy, P_k, and the term T_2 represents the production from the interaction between the mean velocity and the intermittency field. The term T_3 is an additional diffusion-related production term which is kept active over the entire flow field and no blending is applied to this term. The production terms above are given as

$$T_0 = 2C_0\rho\sqrt{u_k u_k}\cdot f(s)f'(s) \qquad (5)$$

$$T_1 = C_1\gamma\frac{P_k}{k} \qquad (6)$$

$$T_2 = C_2\gamma\rho\frac{k^{3/2}}{k\omega}\frac{u_i}{\sqrt{u_k u_k}}\frac{\partial u_i}{\partial x_j}\frac{\partial \gamma}{\partial x_j} \qquad (7)$$

$$T_3 = C_3\rho\frac{k^2}{k\omega}\frac{\partial \gamma}{\partial x_j}\frac{\partial \gamma}{\partial x_j} \qquad (8)$$

The function $f(s)$ was formulated to account for the distributed breakdown. This function depends on the streamline coordinate, which can simply be computed by solving the transport equation of the streamline coordinate, s, in equation (13), or s', in equation (14). The form of this function and its derivation are given as

$$f(s) = \frac{as'^4 + bs'^3 + cs'^2 + ds' + e}{gs'^3 + h} \qquad (9)$$

$$f'(s) = \frac{df(s)}{ds'}\frac{ds'}{ds} = \frac{df(s)}{ds'}\frac{d(s-s_t)}{ds} = \frac{df(s)}{ds'} \qquad (10)$$

The coefficients are

$$a = 50\tilde{n}^{0.5};\quad b = -0.4906;\quad c = 0.204\tilde{n}^{-0.5};\quad d = 0.0;\quad e = 0.04444\tilde{n}^{-1.5};\quad h = 10e;\quad g = 50 \qquad (11)$$

where $\tilde{n} = n\sigma/U$. The spot production rate, $\hat{n}\sigma$, where $\hat{n} = n\nu^2/U^3$, is given by the correlation of Mayle [11] for zero pressure gradient and it has been modified by Suzen and Huang as:

$$\hat{n}\sigma = 1.8\times10^{-11}Tu_\infty^{7/4} \qquad (12)$$

The production term T_0 in equation (5) requires the calculation of the streamwise distance. In order to eliminate the difficulties associated with calculating the streamwise distance, in case of complex geometries, Suzen and Huang developed the transport equation for the streamwise distance s as follows:

$$\frac{\partial \rho u_j s}{\partial x_j} = \rho\sqrt{u_k u_k} + \frac{\partial}{\partial x_j}\left[\left(\frac{\mu+\mu_t}{\sigma_s}\right)\frac{\partial s}{\partial x_j}\right] \qquad (13)$$

and indeed the transition location, s_t, is actually taken as a constant value. Equation (13) can also be derived in the form of s', where $s'=s-s_t$, as follows:

$$\frac{\partial \rho u_j s'}{\partial x_j} = \rho\sqrt{u_k u_k} + \frac{\partial}{\partial x_j}\left[\left(\frac{\mu+\mu_t}{\sigma_s}\right)\frac{\partial s'}{\partial x_j}\right] \qquad (14)$$

The model constants are

$$\sigma_s = 0.1;\quad \sigma_{\gamma l} = \sigma_{\gamma t} = 1.0;\quad C_0 = 1.0;\quad C_1 = 1.6;\quad C_2 = 0.16;\quad C_3 = 0.15 \qquad (15)$$

The transition onset location is determined by the correlation in terms of the freestream turbulence intensity, Tu, and the acceleration parameter, K_t, and the maximum absolute value of that parameter in the downstream deceleration region

$$\mathrm{Re}_{\theta t} = (120 + 150Tu^{-2/3})\coth\left[4(0.3 - 10^5 K_t)\right] \quad (16)$$

In order to employ this intermittency model to successfully simulate the transition, Suzen and Hung suggested that the turbulence model selected to obtain a μ_t must produce fully turbulent feature before the transition location in order to allow the intermittency to have a full control of the transition behaviour. In their work the Menter-SST model satisfies this requirement. The intermittency is incorporated in computations simply by multiplying the eddy viscosity in the diffusive part of the mean flow equation, which is obtained from the turbulence model, by the intermittency factor, γ. The transition model interacts with the turbulence model via the diffusion part of the mean flow equation:

$$\tilde{\mu}_t = \gamma\mu_t \quad (17)$$

It must be noted that γ does not appear in the generation term of the turbulence kinetic energy equations. The computation steps are given as follows: (a) Set (guess) the onset of the transition position, s_t, (the first guess is set at the leading edge point); (b) Solve the mean flow equations: the momentum equations with a modified eddy viscosity, $\tilde{\mu}_t$, and the continuity equation (which is in the form of pressure correction equation); (c) Solve the turbulence transport models: the k-equation, the ω-equation, and then compute the μ_t; (d) Compute the location of the transition onset, s_t, by searching for the point where $\mathrm{Re}_\theta = \mathrm{Re}_{\theta t}$; (e) Solve the equation of the streamwise coordinate s (or s'); and (f) Solve the intermittency transport model.

It should be noted that setting γ to remain between 0.01 and 0.99 at the end of each iteration is necessary to avoid the singularities. The boundary conditions for γ are a zero flux at walls and a fixed small value at the inlet (γ =0.01 is recommended and is used in this work), and the initial condition is set equal to the inlet value. The initial condition of s=0.0 is used all over the flow field, and the gradient of s is set to zero at all boundaries.

2.2 Transport model of Menter et al.

According to Menter et al [4], the transport equation for the intermittency factor is developed based on the idea of dimensionless parameters, which define profiles inside the laminar and turbulent portions of the boundary layer. The relative magnitude of these quantities inside the boundary layer depends on the development stage of the boundary layer and is therefore proportional to the momentum thickness used in the transition correlations. This information can trigger the transition process.

An intermittency equation can be written as

$$\frac{\partial \rho u_j f}{\partial x_j} = P_f - E_f + \frac{\partial}{\partial x_j}\left[\left(\mu + \frac{\mu_t}{\sigma_f}\right)\frac{\partial f}{\partial x_j}\right] \quad (18)$$

with the sources consist of production term, P_f , and destruction term, E_f, defined as follows:

$$P_f = C_{f1}\rho S F_{G1} f \quad (19)$$

$$E_f = C_{f2} P_f f \quad (20)$$

The function F_{G1} is zero upstream of the transition point and is activated at the prescribed $\mathrm{Re}_{\theta c}$, which is given by an experimental correlation as follows:

$$F_{G1} = \max[\tilde{\xi}_1(1 + C_{f3}\xi_2) - 1; 0] \quad (21)$$

$$\tilde{\xi}_1 = \frac{\xi_1}{[1 + (0.5\xi_1)^4]^{0.25}} \quad (22)$$

$$\xi_2 = \frac{1}{0.051\mathrm{Re}_{\theta c}}\frac{\nu_t}{\nu} \quad (23)$$

$$\xi_1 = \frac{1}{2.07\mathrm{Re}_{\theta c}}\frac{S y_n^2}{\nu} \quad (24)$$

For technical reasons, $\tilde{\xi}_1$ is limited to remain between 0 and 2, and the model constants are

C_{f1} = 0.5; C_{f2} = 0.1; C_{f3} = 5.0;

$$\sigma_f = 1.0 \quad (25)$$

The transition model interacts with the turbulence model via the production term of the turbulence kinetic energy, P_k:

$$\tilde{P}_k = F_t P_k \quad (26)$$

The transition (intermittency) function F_t is defined from the non-linear distribution level f as follows:

$$F_t = \frac{\tilde{f}^6}{(\tilde{f} - 0.01)^6 + 1} \quad (27)$$

with $\tilde{f} = \max[2f - 5;\, 0]$. The boundary conditions for f are a zero flux at walls and a fixed small value at the inlet (f=0.01 is used in this work) and the initial condition is set equal to its inlet value.

The computation steps are summarized as follows: (a) Solve the mean flow equations: the momentum equations, and the continuity equation (which is in the form of pressure correction equation); (b) Specify the $\mathrm{Re}_{\theta c}$ with the value corresponding to the requirement of each test case; (c) Solve the turbulence transport models: the k-equation with a modified production, $\tilde{P}_k$, the ω-equation, and then compute the μ_t; and (d) Solve the generalized intermittency transport equation.

3. Numerical Details

Three widely examined test cases: T3AM, T3A and T3B (J. Coupland, Applied Science Lab., Rolls-Royce plc, Derby, England, United Kingdom, Dec. 1993), are considered in the present paper where transition is driven by the external freestream turbulence (bypass transition) rather than by the development of Tollmien-Schlichting (T-S) waves (natural transition). All cases designated are boundary-layer flows on a flat plate with a sharp leading edge under zero-pressure-gradient condition. Details of grid configuration and boundary conditions are shown in Fig. 1.

The computations were performed with an elliptic solver which solved the mean flow, turbulence model, and intermittency model using the second-order TVD-upwind scheme based on Van Leer's flux limiter (Van

Leer, 1979) and the finite volume discretization. In the computations, a range of grid densities was explored by performing a careful grid-dependent check, in which the grid spacing was both decreased by half, and a mesh of 110 (streamwise) × 80 (expanding from wall to the freestream) was adopted for all test cases. In all cases, the near-wall nodes were located at y^+ having values between 0.08 and 0.3. Computations began ahead at x=15 cm upstream of the test plate leading edge. This was vital, because it enabled the uniform profiles of k and ω to be assigned. If one starts computations on the plate itself, the predicted transition point is strongly dependent on the assumptions made about the way k and ω vary across the boundary layer [17]. As a consequence, a considerably reduced streamwise internodal spacing was needed in the vicinity of the leading edge of the plate.

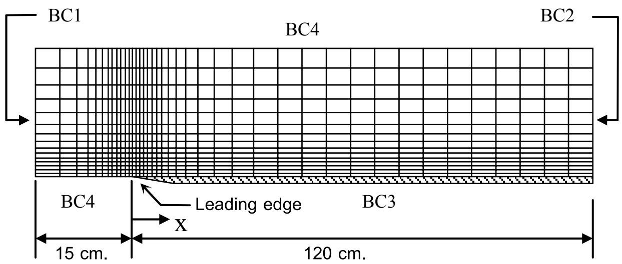

Fig. 1 Grid configuration and boundary conditions

In this work, incompressible flow is considered so that the fluid density and molecular viscosity are set to constant values of 1.2 kg/m^3 and 1.8×10^{-5} kg/m·s respectively. The boundary conditions for BC1, BC2, BC3, and BC4 boundaries are inlet, outlet, no-slip wall and freestream boundary conditions respectively with the following specification:

Freestream: Gradients of all variables with respect to the vertical axis (y) are set to zero.

Wall: No-slip conditions are imposed.

Outlet: Gradients of all variables with respect to the horizontal axis (x) are set to zero.

Inlet: Uniform values of all variables are used.

In all computations, it should be noted that only the zero pressure gradient condition is of interest in this work so that the normal zero gradient of pressure has to be applied for all boundaries. The initial streamwise mean velocity profile is the Blasius velocity profile (δ/x=5.0/Re$^{1/2}$), and the inlet conditions are prescribed to match the experimental decay of the freestream turbulence intensity. In the pretransition region, the experimental measurements reveal that the streamwise fluctuation component is predominately larger than the normal and crossflow components as reported by Savill (1991) and Baek et al [10]

$$\overline{u^2} = u'^2\,,\, \overline{v^2} = v'^2 = 0\,,\quad \overline{w^2} = 0.04u'^2 \qquad (28)$$

and $2k = \overline{u^2} + \overline{v^2} + \overline{w^2} = 1.04u'^2$ so that it is possible to assume $\sqrt{2k} \approx u'$. From this approximation the inlet turbulence kinetic energy is obtained by fixing its value according to the inlet experimental freestream turbulence level, FSTI, and the inlet viscosity ratio, R_μ, is specified in order to match the experimentally measured decay of the freestream turbulence intensity. Hence, the inlet conditions of the turbulence variables are calculated from the following relationships:

$$\mu_t = R_\mu \mu\,;\;\; k = 0.5(FSTI \cdot U_{in})^2\,;\;\; \omega = \rho k/\mu_t \qquad (29)$$

A summary of the inlet conditions for all test cases used in this paper is given in Table 1.

Table 1 Summary of all test case inlet conditions.

Case	U_{in} (m/s)	FSTI (%)	R_μ	$Re_{\theta c}$
T3AM	19.8	0.98	3.0	810
T3A	5.4	3.35	4.0	260
T3B	9.4	6.14	38.5	160

4. Results and Discussion

Two transition models with different intermittency transport equations, the Suzen-Huang model and the Menter et al model, are used to predict the experimental test cases assembled by Coupland (1993): T3AM, T3A and T3B. These experimental data are specially selected to test the capability of transition models to predict the effect of freestream turbulence on the development of transition of a laminar boundary layer under zero pressure gradient condition. Comparisons are also made for all cases between these two transition models and the conventional turbulence models, that is, the Launder-Sharma model, which has been known as the best model among all available two-equation models for analysis of transitional flow, and the Menter-SST model. The test cases are specified with the corresponding test conditions described in Table 1. With these specifications the inlet conditions of turbulence variables were obtained and the decay of freestream turbulence intensity is matched with the experimental data as shown in Fig. 2.

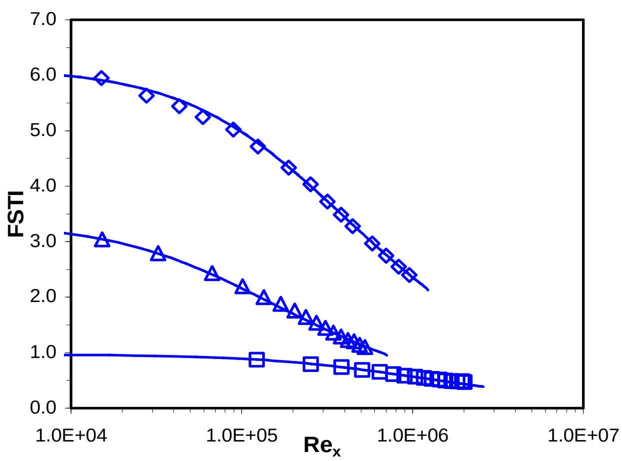

Fig. 2 Comparison of measured freestream turbulence intensity for test cases: T3AM (□), T3A (Δ), T3B (◊) with the numerical results (solid lines)

Fig. 3 displays the predicted and measured skin friction coefficients, the analytic laminar skin friction coefficient, c_f=0.664/Re$^{1/2}$, and the analytic turbulent skin friction coefficient, c_f=0.027/Re$^{1/7}$. The skin friction coefficient plays an important role in indicating where the starting and ending points of transition are. The variation of the skin friction coefficient along the flat plate is usually displayed with respect to the Reynolds number, and the linear-scale plot is displayed in this work. The start and the end of transition occur at the points where skin friction coefficient profile reaches the minimum and maximum values respectively and the profile variation between two those points indicates the growth rate of transition and the length of transition (the more the rapid growth rate the shorter the transition length). In this result, to assess the ability of the models in predicting the onset of transition and the length of transition, the skin friction coefficient profile is therefore an appropriate indicator. As seen in Fig. 3, the Menter-SST model gives the immediate transition to turbulence at the leading edge of the flat plate showing almost no laminar zone for all three test cases. The Launder-Sharma model gives early onsets of transition and the transition to turbulence grows up too rapidly when compared to the experimental data, and hence a shorter transition length. The prediction of the Menter et al model gives the result nearly the same as the Launder-Sharma model in T3AM case, and delayed transition onsets with the under-predicted skin friction coefficients at the end of the transition region in both T3A and T3B cases. The Suzen- Huang model shows better agreement with the experimental data in T3A case and the too early onset of transition in T3AM case but in T3B case this model predicted the too delayed onset of transition and the slightly overshoot skin friction coefficient at the end of the transition region.

The predicted shape factor variations are compared with the experimental data in Fig. 4. The shape factor is defined as the ratio of the displacement thickness to the momentum thickness in the boundary layer, and hence it describes the influence of the freestream turbulence eddies on transition. Moreover it indicates if the boundary layer is separated or has the tendency to separate. A large shape factor implies that the boundary layer separation is about to occur. It has been known that, from analysis, the shape factor is about 2.6 for the laminar boundary layer and about 1.4 for the turbulent boundary layer and varies between these two values for the transitional boundary layer. In Fig. 4, it must be noted that all presented models predict a laminar flow characteristic before the transition onset point and show a turbulent flow characteristic after the end of the transition region. Menter-SST model gives an immediate decay of shape factor at the leading edge of the flat plate for all three test cases. This implies that this model produces fully turbulent feature and cannot detect any effects of transition. With the Launder-Sharma model, the predicted shape factor profile appears to match the experimental data better than that of the other presented models. This is a coincidence. These results merely reflect the fact that the k-ε model predicts an early flow transition [7] as can be seen in Fig. 3. For the Menter et al and Suzen-Huang models, the computed shape factor distribution are widely spread and also become the laminar value of 2.6 from the leading edge of the flat plate toward the transition onset. In T3AM case, all the presented models give unsatisfactory results, the predicted profiles drop down too early from the experimental data. For T3A case, the laminar shape factors of approximately 2.6 of both models and of experiment are completely ended at the stations of $Re_x= 2.08\times10^5$, 1.64×10^5, and 1.35×10^5, respectively, and $Re_x=9.80\times10^4$, 1.04×10^5, and 5.91×10^4 in T3B case, respectively. The difference between the predicted results and experimental data, the prediction larger than the experimental data, implies that both models predict the delayed onset of transition. Moreover, the rapid decay of the shape factor profiles from laminar to turbulence regions leads to the shorter transition length.

Fig. 5 shows the intermittency profiles predicted by the Suzen-Huang model at various streamwise stations inside the transition zone. As can be seen, for T3A case, the profiles exhibit a peak between $y/\delta^*=0.5$ and $y/\delta^*=1.5$, then drop off toward zero near the edge of the boundary layer, around $y/\delta^*=8.0$. For T3B case, the profiles display the same characteristics as found in T3A case, but due to a higher freestream turbulence intensity, the results show that the peaks of the profiles are less pronounced for this case and the spread of the intermittency appears wider across the transition region. For T3AM case, it should be noted that this case has a lower freestream turbulence intensity than T3A and T3B. As a result, the profiles show more pronounced peaks and the spread of the intermittency is narrow in the transition zone. Fig. 6 shows the generalized intermittency profiles predicted by the Menter et al model. It is clear that the profile characteristics are quite different from those of the Suzen-Huang model. The intermittency function of this model is designed to focus on the boundary layer edge by being unity through the transition region toward downstream. At any streamwise station inside the transition zone, the profiles start and grow up rapidly toward unity and therefore spread across the boundary layer and then decay rapidly toward zero afterward. In all cases, the profiles exhibit a peak between $y/\delta^*=1$ and $y/\delta^*=2$, then drop off toward zero near the edge of the boundary layer, around $y/\delta^*=5.5$ for T3AM, $y/\delta^*=5.5$ for T3A, and $y/\delta^*=10$ for T3B.

5. Conclusion

Two transition models with the intermittency transport equation are implemented and their ability are assessed. The first one is the Suzen-Huang model interacts with the turbulence model via the diffusion part of the mean flow equations and the other one is the Menter et al model interacts with the turbulence model via the production term of the turbulence kinetic energy, P_k. Both models are used in conjunction with Menter-SST model to predict the flat plate boundary-layer flow with zero pressure gradient and three different freestream turbulence intensities corresponding to the conditions of T3AM, T3A and T3B experiments by Coupland (1990). Performance of both models are assessed by validating the predicted skin friction coefficient and shape factor results with the experimental data and comparing them with the results of the Launder-Sharma model and of the Menter-SST model.

In case of the skin friction coefficient, the computational results show that the Menter-SST model produces turbulence at the leading edge of the flat plate without capturing any transition effect and the Launder-Sharma model predicts early onsets of transition and a shorter transition length. The Suzen-Huang model predicts the experimental data well only in case of T3A. The Menter et al model predicts unsatisfactorily onsets of transition in all three test cases.

In case of the shape factor, the computation results show that the Menter-SST model produces turbulence thoroughly and therefore neither laminar zone and nor separation appears. The Launder-Sharma model gives the fairly good prediction when compared with other presented models. Both the Suzen-Huang model and the Menter et al model predict unsatisfactorily onsets of transition in all three test cases.

The advantages/disadvantages of both models are summarized as follows:

<u>Menter et al model:</u>

Advantages: (1) The interaction with the turbulence model is stable; (2) The transition location is obtained in a reasonable number of iteration; (3) The model is not activated in stagnation regions where the strain rate magnitude, *S,* is not zero; (4) The solution is independent of the initial condition.

Disadvantages: (1) The model cannot be activated by the turbulence effect in the freestream; (2) The constant $Re_{\theta c}$ must be known before computing.

<u>Suzen and Huang model:</u>

Advantages: (1) The interaction with the turbulence model is stable; (2) The solution is independent of the initial condition.

Disadvantages: (1) The model cannot be activated by the turbulence effect in the freestream; (2) In general, especially for complex flows, the transport equation of streamwise coordinate has to be solved additionally.

Acknowledgments

This research is supported by Thailand Research Fund (TRF) for the Senior Scholar Prof. Pramote Dechaumphai, and the authors would like to thank Dr. Y.B. Suzen, Dr. F.R. Menter, Koen Lodefier and Rene Pecnik for their helpful discussion during the course of this work.

References

[1] Y.B. Suzen, and P.G. Huang, “Modeling of flow transition Using an intermittency transport equation”, J. Fluid Engineering, Vol.122, 2000, pp. 273-284.

[2] J.R. Cho, and M.K. Chung, “A k-ε-γ equation turbulence model”, J. Fluid Mechanics, Vol. 237, 1992, pp. 301-322.

[3] J. Steelant, and E. Dick, “Modelling of bypass transition with conditioned Navier-Stokes equations coupled on an intermittency transport equation”, Int. J. Numer. Methods Fluids, Vol. 23, 1996, pp.193-220.

[4] F.R. Menter, T. Esch, and S. Kubacki, “Transition modelling based on local variables”, Engineering Turbulence Modelling and Experiments-5, W. Rodi and N. Fueyo (Editor), 2002, pp. 555-564.

[5] F.R. Menter, “Two-equation eddy-viscosity turbulence models for engineering applications”, AIAA Journal, Vol. 32, No. 8, 1994, pp. 1598-1605.

[6] B.E. Launder, and B. Sharma, “Application of the energy dissipation model of turbulence to the calculation of flow near a spinning disk”, Letters in Heat and Mass Transfer, Vol. 1, No. 2, 1974, pp.131-138.

[7] Y.B. Suzen, and P.G. Huang, “Predictions of separated and transitional boundary layers under low-pressure turbine airfoil conditions using an intermittency transport equation”, AIAA 2001-0446, 39th AIAA Aerospace Sciences Meeting & Exhibit, Reno, Nevada, January 8-11, 2001.

[8] S. Lardeau, N. Li, and M.A. Leschziner, “LES of transitional boundary layer at high free-stream turbulence intensity, and implications for RANS modelling”, 2005, pp. 431-436.

[9] R.B. Langtry, and F.R. Menter, “Transition modeling for general CFD applications in aeronautics”, AIAA 2005-522, 2005.

[10] S.G. Baek, and M.K. Chung, “ k-ε Model for predicting transitional boundary-layer flows under zero-pressure gradient”, AIAA, Vol. 39, No. 9, 2001, pp. 1699-1705.

[11] R.E. Mayle, “The role of laminar-turbulent transition in gas turbine engines”, ASME J. Turbomach, Vol. 113, pp. 509-537.

[12] B.J. Abu-Ghannam, and R. Shaw, “Natural transition of boundary layer: The effects of turbulence, pressure gradient, and flow history”, J. Mech. Engng. Sci., Vol. 22, No. 5, 1980, pp. 213-228.

[13] S. Dhawan, and R. Narasimha, “Some properties of boundary layer during the transition from laminar to turbulent flow motion”, J. Fluid Mechanics, Vol. 3, pp. 418-436.

[14] R.Pecink, W. Sanz, A. Gehrer, and J. Woisetschlager, “Transition modeling using two different intermittency transport equation”, Flow, Turbulence and Combustion, Vol. 70, 2003, pp. 299-323.

[15] K. Lodefier, B. Merci, C. De Langhe, and E. Dick, “Transition modeling with the SST turbulence model and intermittency transport equation”, ASME Turbo Expo, Atlanta, Georgia, USA, June 16-19, 2003.

[16] Y.B. Suzen, and P.G. Huang, “Numerical simulation of transitional flows as affected by passing wakes”, AIAA 2004-0103, 42nd AIAA Aerospace Sciences Meeting & Exhibit, Reno, Nevada, January 5-8, 2004.

[17] T.J. Craft, B.E. Launder, and K. Suga, “Prediction of turbulence transition phenomena with a nonlinear eddy-viscosity model”, Int. J. Heat and Fluid Flow, Vol. 18, 1997, pp. 15-28.

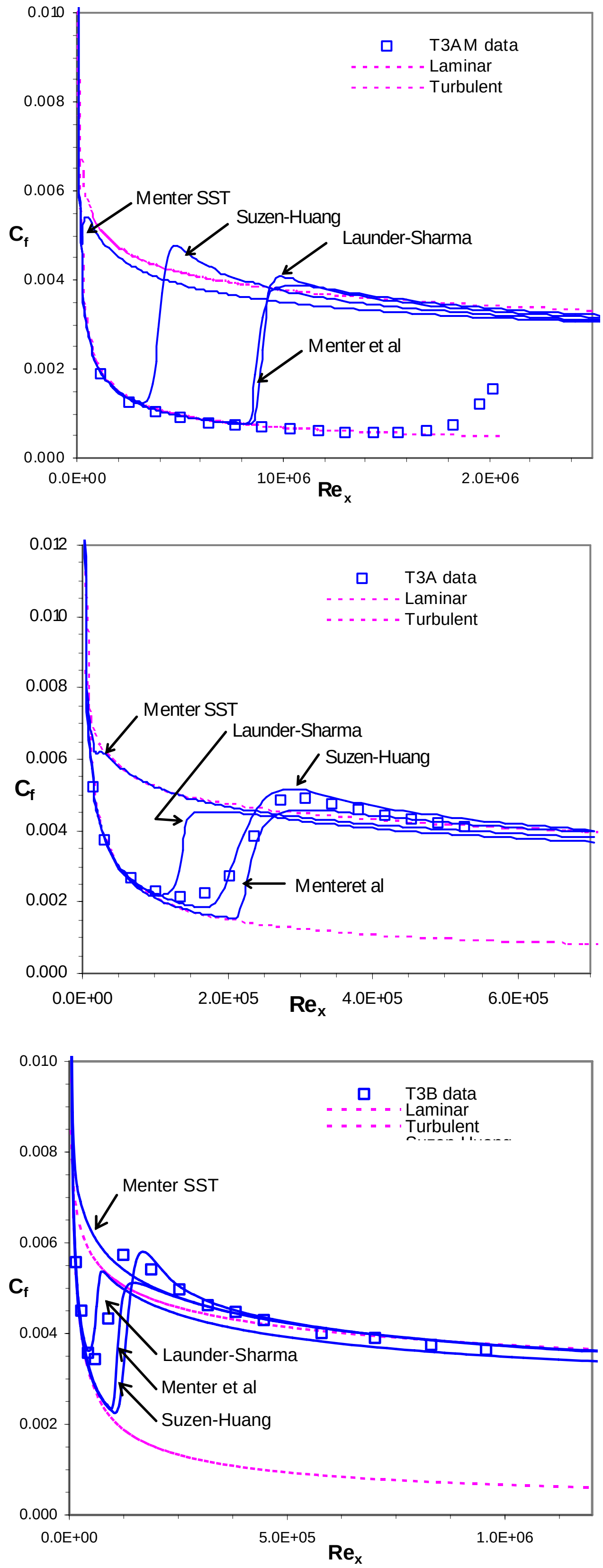

Fig. 3 Comparison of skin friction coefficient for T3AM (top), T3A (middle) and T3B (bottom)

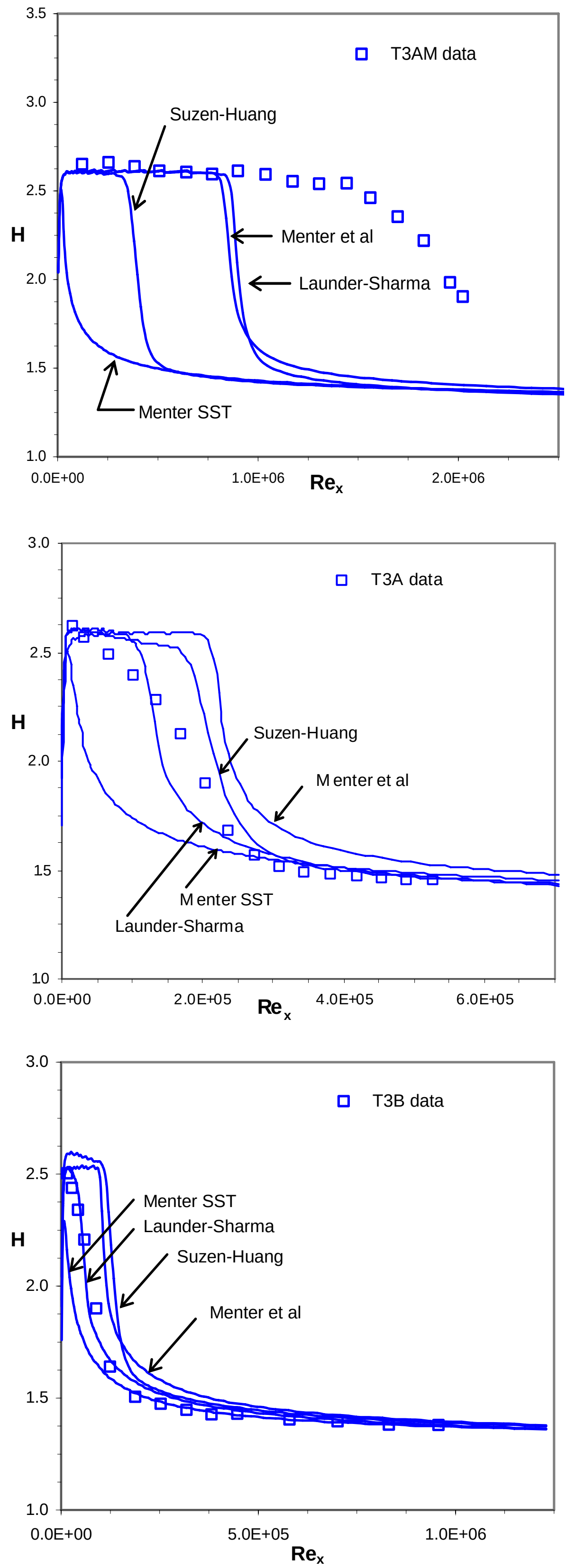

Fig. 4 Comparison of shape factor for T3AM (top), T3A (middle) and T3B (bottom)

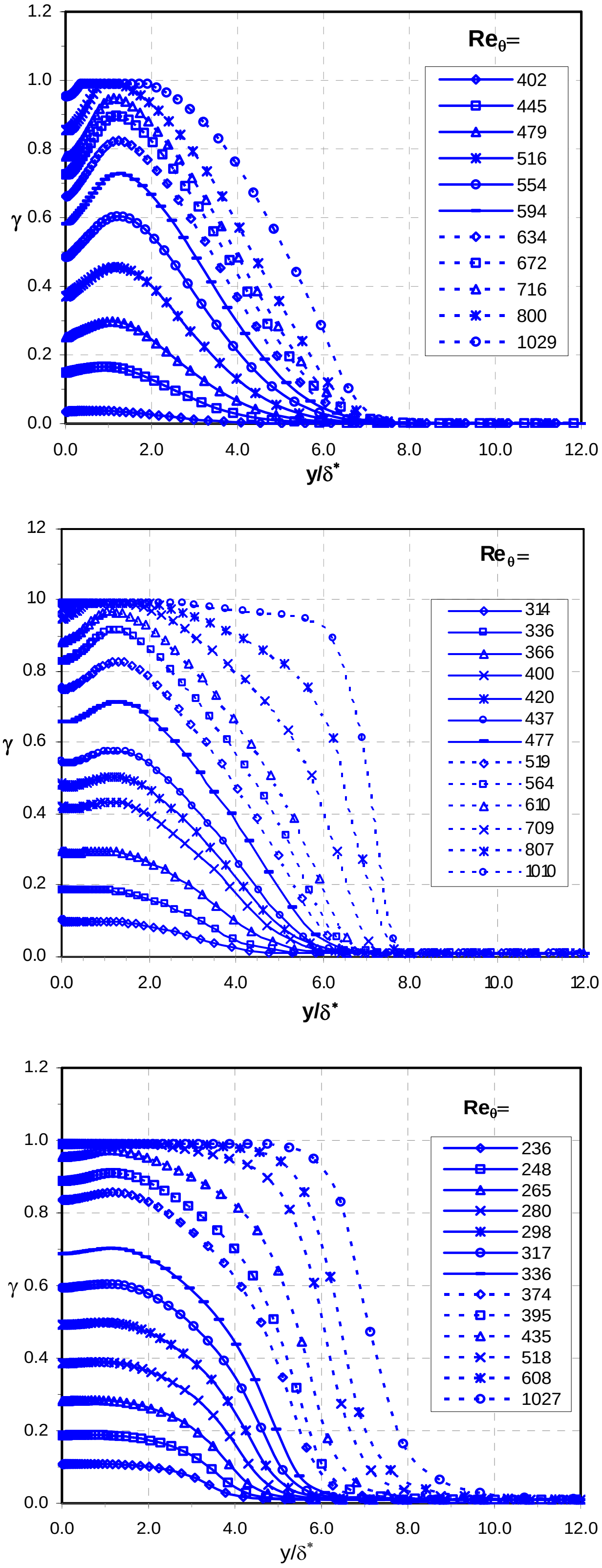

Fig. 5 Intermittency factor profiles of Suzen and Huang model for T3AM (top), T3A (middle) and T3B (bottom) cases

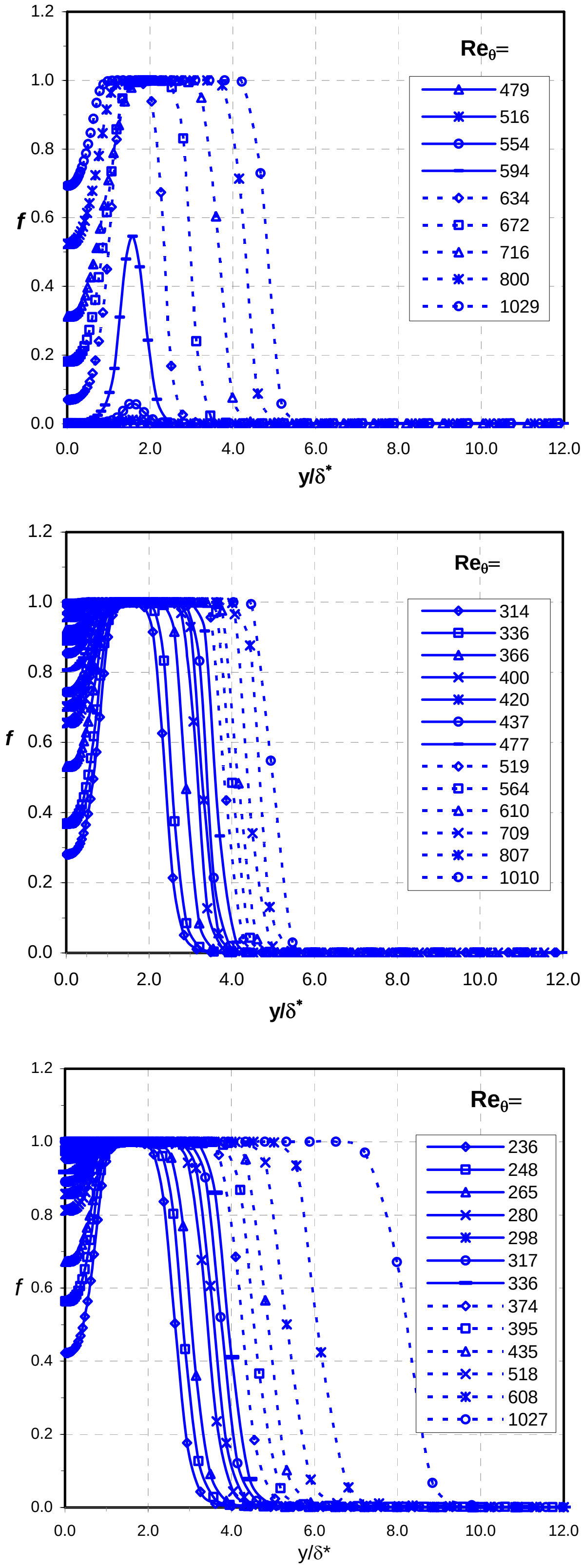

Fig. 6 Generalized intermittency factor profiles of Menter et al model for T3AM (top), T3A (middle) and T3B (bottom) cases